

# Electrochemical Synthesis and Characterization of the Single-Electron Oxidation Products of Ferric Porphyrins

Martin A. Phillippi and Harold M. Goff\*

Contribution from the Department of Chemistry, University of Iowa, Iowa City, Iowa 52242.  
Received June 26, 1981

**Abstract:** High-spin iron(III) porphyrins are oxidized by electrochemical and selected chemical methods. Both monomeric chloro complexes and  $\mu$ -oxo dimeric species have been examined. Products are isolated as perchlorate salts in analytically pure form in favorable cases. Contrary to previous interpretations, the singly oxidized species are better formulated as iron(III) porphyrin  $\pi$ -cation radicals rather than as iron(IV) complexes. This finding is based on electrochemical measurements, electronic absorption spectra, NMR spectra, infrared spectra, and Mössbauer measurements. Oxidation potentials for diverse anionic complexes of iron(III) tetraphenylporphyrin are essentially constant at  $1.10 \pm 0.02$  V (SCE), suggestive of porphyrin-centered rather than metal-centered oxidation. Electronic absorption spectra exhibit broad bands at long wavelength, not unlike those for known  $\pi$  radicals. Unusually large NMR paramagnetic shifts for phenyl protons of oxidized iron tetraphenylporphyrin derivatives are rationalized by proton-radical couplings previously measured for zinc  $a_{2u}$  porphyrin radicals. The oxidized iron octaethylporphyrin complex is better described as an  $a_{1u}$  species. Efficient relaxation of electron spin by the paramagnetic iron center permits well-resolved NMR spectra. Infrared spectra serve to demonstrate integrity of the oxo linkage in oxidized  $\mu$ -oxo dimers. A new absorption band near  $1280\text{ cm}^{-1}$  is seemingly diagnostic of porphyrin-centered oxidation of tetraphenylporphyrin metal complexes. Mössbauer spectra reveal little perturbation of charge at the iron center associated with oxidation. Isomer shift values near  $0.4\text{ mm/s}$  (iron metal) resemble those for parent iron(III) complexes. Solution magnetic moment measurements yield an unusual  $5.5\text{-}\mu_B$  value for oxidized iron tetraphenylporphyrin and iron octaethylporphyrin derivatives. Absence of metal-centered oxidation for weak-field anionic complexes indirectly supports the necessity of an oxo or hydroxo ligand in iron(IV) states of hemoproteins.

## Introduction

Aerobic organisms are continuously exposed to a strongly oxidizing environment of molecular oxygen and to smaller amounts of peroxide species. The ability to utilize oxygen in respiration and metabolism must therefore be coupled with protective mechanisms that prevent indiscriminate destruction of cellular components. The threat posed to living cells by reactive superoxide and peroxide species is averted by enzymes that effectively scavenge these strongly reducing and oxidizing substrates.

Both peroxidase and catalase degrade hydrogen peroxide and organic peroxides through a catalytic cycle that apparently involves oxidation of the heme prosthetic group to the iron(IV) state.<sup>1-3</sup> Two electron oxidation of resting ferric horseradish peroxidase (HRP) generates the green compound I. One equivalent reduction yields the red compound II. Mössbauer results are consistent with an iron(IV) configuration in both molecules.<sup>4</sup> By analogy, the oxygen activation cycle of cytochrome P-450 yields intermediates with formal iron(IV) and/or radical character.<sup>5,6</sup> The second oxidation equivalent in compound I is thought to reside as a porphyrin  $\pi$ -cation radical.<sup>7,8</sup> In doubly oxidized cytochrome *c* peroxidase, on the other hand, the second oxidation equivalent is observable in the ESR and ENDOR spectra as a protein (probably methionine) free radical.<sup>9</sup>

Porphyrin ring oxidation (vs. metal oxidation) is apparent in other classes of hemoproteins. Thus, the iron isobacteriochlorin prosthetic groups of nitrite and sulfite reductases exhibit relatively low oxidation potentials that are thought to represent formation of iron(III)  $\pi$ -cation radical species.<sup>10,11</sup>

One-electron oxidation of iron(III) porphyrins yields products that may serve as active-site models for oxidized hemoprotein intermediates. Wolberg and Manassen reported preparative electrochemical oxidation of a variety of metalloporphyrins and noted that iron(III) porphyrins oxidized in benzonitrile solution yielded (an incompletely-characterized) low-spin iron(III) porphyrin  $\pi$ -cation radical species.<sup>12</sup> Felton et al. obtained products from electrochemical oxidation of iron(III) porphyrins in chlorinated solvents.<sup>13,14</sup> On the basis of spectroscopic and magnetic measurements, high-spin iron(IV) states were assigned.

Generation of oxidized iron porphyrin species by chemical oxidants has also been reported. Groves<sup>6,15</sup> and Chang<sup>16</sup> have independently shown that iodosylbenzene derivatives react with iron porphyrins and alkenes or alkanes to yield epoxides or alcohols. A transient intermediate analogous to HRP compound I was optically detected.<sup>16</sup> More recently, Groves et al. have examined the iron porphyrin products generated by *in situ* oxidation with iodosylbenzene or *m*-chloroperoxybenzoic acid at  $-78^\circ\text{C}$ .<sup>15b</sup> Mössbauer isomer shift values very near  $0.0\text{ mm/s}$  are convincing in terms of an iron(IV) formulation. The *m*-chloroperoxybenzoic acid oxidant yields a species best described as an iron(IV)  $\pi$ -cation radical, as judged by the large porphyrin *meso*-phenyl proton NMR shift values. Magnetic and NMR spectral differences between species prepared by the two chemical oxidants remain to be explained. Reactivity patterns and facile

(1) Hanson, L. K.; Chang, C. K.; Davis, M. S.; Fajer, J. *J. Am. Chem. Soc.* **1981**, *103*, 663-670.

(2) Dunford, H. B.; Stillman, J. S. *Coord. Chem. Rev.* **1976**, *19*, 187-251.

(3) Hewson, W. D.; Hager, L. P. "The Porphyrins"; Dolphin, D., Ed.; Academic Press: New York, 1979; Vol. 7, pp 295-332.

(4) (a) Moss, T. H.; Ehrenberg, A.; Bearden, A. J. *Biochemistry* **1969**, *8*, 4159-4162. (b) Harami, T.; Maeda, Y.; Morita, Y.; Trautwein, A.; Gonser, U. *J. Chem. Phys.* **1977**, *67*, 1164-1169. (c) Schulz, C. E.; Devaney, P. W.; Winkler, H.; Debrunner, P. G.; Doan, N.; Chiang, R.; Rutter, R.; Hager, L. P. *FEBS Lett.* **1979**, *103*, 102-105.

(5) Chang, C. K.; Dolphin, D. "Bioorganic Chemistry"; Van Tamelen, E. E., Ed.; Academic Press: New York, 1978; Vol. 4, pp 37-80.

(6) Groves, J. T.; Kruper, W. J.; Nemo, T. E.; Myers, R. S. *J. Mol. Catal.* **1980**, *7*, 169-177.

(7) (a) Dolphin, D.; Felton, R. H. *Acc. Chem. Res.* **1974**, *7*, 26-32. (b) Dolphin, D.; Addison, A. W.; Cairns, M.; Dinello, R. K.; Farrell, N. P.; James, B. R.; Paulson, D. R.; Welborn, C. *Int. J. Quantum Chem.* **1979**, *16*, 311-329.

(8) Roberts, J. E.; Hoffman, B. M.; Rutter, R.; Hager, L. P. *J. Biol. Chem.* **1981**, *256*, 2118-2121.

(9) Hoffmann, B. M.; Roberts, J. E.; Brown, T. G.; Kang, C. H.; Margoliash, E. *Proc. Natl. Acad. Sci. U.S.A.* **1979**, *76*, 6132-6136.

(10) Stolzenberg, A. M.; Spreer, L. O.; Holm, R. H. *J. Am. Chem. Soc.* **1980**, *102*, 364-370.

(11) Chang, C. K.; Fajer, J. *J. Am. Chem. Soc.* **1980**, *102*, 848-851.

(12) Wolberg, A.; Manassen, J. *J. Am. Chem. Soc.* **1970**, *92*, 2982-2991.

(13) Felton, R. H.; Owen, G. S.; Dolphin, D.; Fajer, J. *J. Am. Chem. Soc.* **1971**, *93*, 6332-6334.

(14) Felton, R. H.; Owen, G. S.; Dolphin, D.; Forman, A.; Borg, D. C.; Fajer, J. *Ann. N. Y. Acad. Sci.* **1973**, *206*, 504-514.

(15) (a) Groves, J. T.; Nemo, T. E.; Myers, R. S. *J. Am. Chem. Soc.* **1979**, *101*, 1032-1033. (b) Groves, J. T.; Haushalter, R. C.; Nakamura, M.; Nemo, T. E.; Evans, B. J. *Ibid.* **1981**, *103*, 2884-2886.

(16) Chang, C. K.; Kuo, M.-S. *J. Am. Chem. Soc.* **1979**, *101*, 3413-3415.

$\text{H}_2^{18}\text{O}$  exchange suggest a ferryl linkage,  $\text{Fe}^{\text{IV}}=\text{O}$ .

In a promising approach toward generation of the putative ferryl species, Chin, Balch, and La Mar have performed reactions with ligating bases and the ( $\mu$ -peroxo)iron(III) porphyrin dimer.<sup>17,18</sup> The dimer is cleaved by base, B, to yield at low temperature a species spectroscopically characterized as  $(\text{B})\text{PFe}^{\text{IV}}=\text{O}$ .<sup>17</sup> Oxidation of triphenylphosphine by the active complex has been demonstrated.<sup>19</sup>

Generation and evaluation of suitable models for the putative high oxidation states of hemoproteins remains as an active, challenging, and difficult area of metalloporphyrin chemistry. The approach taken in this study has involved primarily electrochemical synthetic methods, with evaluation of selected chemical oxidants. Isolation of both oxidized monomeric and  $\mu$ -oxo dimeric iron porphyrins of high redox purity has been possible by modification of published techniques. Solution properties have been investigated in detail by NMR methods. Although a complete description of the electronic structure is not yet possible, it will be shown that singly oxidized iron(III) porphyrin chloride complexes are better described as  $\pi$ -cation radical species,  $\text{PFe}^{\text{III}}\text{Cl}^+$ , than as iron(IV) complexes. This conclusion is consistent with our recent electrochemical study of iron(III) porphyrin oxidations.<sup>20</sup> The  $\pi$ -radical formulation was also arrived at independently for chemically oxidized complexes, and preliminary results were reported during preparation of this manuscript.<sup>21</sup>

### Experimental Section

**Materials.** Iron(III) porphyrin chloride complexes were prepared by standard literature methods.<sup>22-24</sup> Compounds were routinely characterized by thin-layer chromatography, elemental analysis, and proton and carbon-13 NMR spectroscopy. Octaethylporphyrin (OEP) was deuterated at the meso positions by reflux with *p*-toluenesulfonic acid-*d*<sub>1</sub> in *o*-dichlorobenzene.<sup>25</sup> Solvents were purified by published procedures<sup>26</sup> and stored over molecular sieves. Methylene chloride and chloroform were routinely purified by washing with 1 M  $\text{Na}_2\text{CO}_3$  solution, washing with water, drying over solid  $\text{Na}_2\text{CO}_3$ , and distilling. Chlorinated solvents were stored over 3-Å molecular sieves and protected from light. Purified chloroform was purged with nitrogen and refrigerated. Failure to remove HCl and trace impurities from chlorinated solvents results in splitting  $\mu$ -oxo dimers and reduction of oxidized compounds.

**Electrochemical Oxidations.** Synthetic scale electrochemical oxidations were performed in a three-electrode cell. Counter and reference electrodes were separated from the bulk solution through use of fine glass frits. Both electrodes consisted of silver wires immersed in the same supporting electrolyte (0.1 M) and solvent employed in the bulk solution. A standard cylindrical platinum gauze working electrode was utilized. An argon stream was passed through the solution for mixing purposes as well as to maintain an inert atmosphere (primarily to exclude water). The solution was also magnetically stirred to promote mixing. The iron porphyrin (~100 mg) was dissolved in 100 mL of solvent containing 0.1 M supporting electrolyte. Oxidation potentials were determined with respect to the silver wire reference by cyclic voltammetric measurements in the preparative cell. A potential anodic of the wave of interest, but cathodic of the next oxidation wave was utilized. Initial currents of 30–100 mA gradually dropped to approximately one percent of the original value in typically 25 min. During electrolysis and subsequent isolation work the electrolysis solution was protected from light to prevent any possible photochemical reactions. Solid products were stored desiccated at  $-20^\circ\text{C}$ . Final products stored in this manner showed no

appreciable reduction over a period of 3 years. Solutions of oxidized iron porphyrins exhibit spontaneous reduction to the iron(III) form. For purified methylene chloride solutions (protected from light, at room temperature) half lives for reduction range from perhaps a few hours for monomeric species to a few weeks for the singly oxidized  $\mu$ -oxo dimer.

**Caution!** We have not experienced detonation of the iron porphyrin perchlorate adducts described here, but caution is urged when handling any organic perchlorate compound. Descriptions of specific preparations follow.

$(\text{TPP})\text{Fe}_2\text{O}(\text{ClO}_4)_2$ . The two-electron oxidation product of iron(III) tetrabutylporphyrin  $\mu$ -oxo dimer,  $(\text{TPP})\text{Fe}_2\text{O}$ , was carried out by two separate methods.

**Procedure 1.**  $(\text{TPP})\text{Fe}_2\text{O}$  (150 mg) was dissolved in 100 mL of a methylene chloride-acetone (3:1) solution which was 0.1 M in  $\text{LiClO}_4$ . A potential of 1.2 V was applied (vs. the silver wire reference). The initial current of 30 mA dropped to 0.2 mA in 25 min. The solution was reduced in volume by rotary evaporation to ~5 mL, 20 mL of acetone was added, and the solvent was removed under vacuum until about 10 mL of solution remained. The resulting solid was separated by medium glass frit filtration and washed with acetone (5 mL) and ethyl ether (5 mL). Initially some brown material was washed through with the ether, but toward the end the wash was clear. The solid was vacuum dried for 3 h at room temperature. A black microcrystalline product was obtained (77-mg yield).

**Procedure 2.** To methylene chloride (80 mL) which was 0.1 M in tetrabutylammonium perchlorate ( $\text{Bu}_4\text{NClO}_4$ ) was added 135 mg of  $(\text{TPP})\text{Fe}_2\text{O}$ . Electrolysis at 1.1 V gave an initial current flow of 62 mA that decreased to 0.6 mA in 20 min. The methylene chloride was removed by rotary evaporation to a volume of ~10 mL during which time 35 mL of acetone was slowly bled into the mixture. The precipitated, oxidized complex was separated by filtration through a medium-frit glass filter, washed with acetone (5 mL) and ethyl ether (5 mL), and vacuum dried for 3 h. A yield of 65 mg was obtained.

Attempted electrolysis of  $\mu$ -oxo dimers using methylene chloride-acetonitrile (3:1) containing 0.1 M  $\text{LiClO}_4$  always resulted in a mixture of complexes (as verified by proton NMR spectroscopy). This was attributed to the presence of a coordinating solvent which split the  $\mu$ -oxo linkage by coordination to the iron. Hence, coordinating solvents were avoided in all dimer oxidations.

$(\text{TPP}(p\text{-OCH}_3)\text{Fe}_2\text{O}(\text{ClO}_4)_2$ . Synthesis was accomplished by procedure 2 as described above. The utility of procedure 1 for the preparation of  $(\text{TPP}(p\text{-OCH}_3)\text{Fe}_2\text{O}(\text{ClO}_4)_2$  has not been verified. The doubly oxidized dimer has also been successfully recrystallized by dissolution of the solid in a minimum amount of  $\text{CH}_2\text{Cl}_2$  followed by addition of acetone while the solvent was evaporated under a stream of nitrogen (in a dry atmosphere to prevent water condensation).

$(\text{TPP})\text{Fe}_2\text{O}(\text{ClO}_4)$  and  $(\text{TPP}(p\text{-OCH}_3)\text{Fe}_2\text{O}(\text{ClO}_4)$ . Syntheses were performed in the same manner. The appropriate dimer (100 mg) was dissolved in  $\text{CH}_2\text{Cl}_2$  (100 mL) which was made 0.1 M in  $\text{Bu}_4\text{NClO}_4$ . Electrolysis at the first wave (~0.6 V) and subsequent rotary evaporation of solvent while  $\text{CH}_3\text{OH}$  was bled into the mixture allowed recovery of 60 mg of singly oxidized dimer which was vacuum dried for several hours at room temperature. Although this preparation yields the singly oxidized dimer, the product is slowly reduced by methanol in solution. The success of the isolation is due to the solubility of the iron(III) material vs. the insolubility of the oxidized complex in the  $\text{CH}_2\text{Cl}_2$ - $\text{CH}_3\text{OH}$  mixture.

A very efficient procedure for the preparation of  $(\text{TPP})\text{Fe}_2\text{O}(\text{ClO}_4)$  as the toluene solvate was devised on the basis of reduction of the doubly oxidized species with parent iron(III) dimer. The doubly oxidized dimer,  $(\text{TPP})\text{Fe}_2\text{O}(\text{ClO}_4)_2$  (90 mg), was isolated as described above and vacuum dried for several hours. This solid and 70 mg of  $(\text{TPP})\text{Fe}_2\text{O}$  were mixed and dissolved in a minimum amount of methylene chloride-toluene (60:40, 250 mL required). The solution was placed in a 600-mL beaker and covered with aluminum foil containing several small holes, and a 1-L beaker was placed over the smaller beaker. Slow evaporation of solvent over a period of 1 week yielded 82 mg of needlelike crystals which were recovered by filtration and washed with 25 mL of toluene and air dried. One molecule of toluene per dimer unit is retained in the crystal on the basis of elemental analysis and NMR integrations. Although the product appeared to be well suited for X-ray crystallographic studies, the needlelike crystals did not diffract well.

$(\text{OEP})\text{Fe}_2\text{O}(\text{ClO}_4)$ . The iron(III) dimer,  $(\text{OEP})\text{Fe}_2\text{O}$  (50 mg), in 80 mL of methylene chloride-acetone (3:1) solution containing 0.1 M  $\text{LiClO}_4$  was oxidized at 0.75 V. After 30 min the current had dropped sufficiently, and the solution was reduced to a volume of 8 mL by rotary evaporation. The solution was placed in liquid nitrogen for 15 s and rapidly filtered. The brown solid was vacuum dried for 6 h (30-mg yield). This product is contaminated with approximately 35% of an iron(III) complex of unknown structure (vide infra).

(17) Chin, D. H.; Balch, A. L.; La Mar, G. N. *J. Am. Chem. Soc.* **1980**, *102*, 1446-1448.

(18) Chin, D. H.; La Mar, G. N.; Balch, A. L. *J. Am. Chem. Soc.* **1980**, *102*, 4344-4350.

(19) Chin, D. H.; La Mar, G. N.; Balch, A. L. *J. Am. Chem. Soc.* **1980**, *102*, 5945-5947.

(20) Phillippi, M. A.; Shimomura, E. T.; Goff, H. M. *Inorg. Chem.* **1981**, *20*, 1322-1325.

(21) Gans, P.; Marchon, J.-C.; Reed, C. A.; Regnard, J.-R. *Nouv. J. Chim.* **1981**, *5*, 203-204.

(22) Adler, A. D.; Longo, F. R.; Finarelli, J. D.; Goldmacher, J.; Assour, J.; Korsakoff, L. *J. Org. Chem.* **1967**, *32*, 476.

(23) Adler, A. D.; Longo, F. R.; Varadi, V. "Inorganic Synthesis"; Basolo, F., Ed.; McGraw-Hill: New York, 1976; Vol. 16, pp 213-220.

(24) Fuhrhop, J.-H.; Smith, K. M. "Porphyrins and Metalloporphyrins"; Smith, K. M., Ed.; Elsevier: Amsterdam, 1975; pp 765-769.

(25) Smith, K. M.; Langry, K. C.; De Ropp, J. S. *J. Chem. Soc., Chem. Commun.* **1979**, 1001-1003.

(26) Perrin, D. D.; Aramego, W. L. F.; Perrin, D. R. "Purification of Laboratory Chemicals"; Pergamon Press: Long Island City, NY, 1966.

**TPP(*p*-OCH<sub>3</sub>)FeCl(ClO<sub>4</sub>).** Oxidation of TPP(*p*-OCH<sub>3</sub>)FeCl (140 mg) at the first oxidation wave was performed in methylene chloride-acetonitrile (3:1, 80 mL) with 0.1 M LiClO<sub>4</sub> as supporting electrolyte. An applied potential of 1.05 V yielded an initial current of 100 mA. Twenty minutes later the current had dropped to 0.5 mA at which point the solvent was removed by rotary evaporation to a volume of ~5 mL. Methylene chloride (25 mL) was gradually bled in to maintain a constant 5-mL volume, and the evaporation was continued for approximately 10 min. Filtration served to remove part of the LiClO<sub>4</sub>. The filtrate was diluted to 10 mL with methylene chloride and reduced in volume by rotary evaporation while ethyl ether slowly was bled in. If the product oiled out, more methylene chloride was added until a homogeneous solution resulted. Ethyl ether was then slowly added until a precipitate appeared. When a precipitate was observed (~5 mL of ether added), the solution was filtered and the solid product was washed with 5 mL of ether. The solid was dissolved in a minimum amount of methylene chloride and recrystallized by the addition of ethyl ether (under a nitrogen atmosphere). The solid was separated by filtration and vacuum dried for 3 h yielding 41 mg of TPP(*p*-OCH<sub>3</sub>)FeCl(ClO<sub>4</sub>).

**(TPP)FeCl(ClO<sub>4</sub>).** Iron(III) tetraphenylporphyrin chloride (75 mg) was dissolved in methylene chloride (100 mL) which was 0.1 M in tetrapropylammonium perchlorate (Pr<sub>4</sub>NClO<sub>4</sub>). The applied current dropped from 33 to 0.4 mA in 30 min. Rotary evaporation of the solution while bleeding in benzene resulted in precipitation of Pr<sub>4</sub>NClO<sub>4</sub> which was removed by filtration. Pentane (~30 mL) was slowly added dropwise to the filtrate (~10 mL) under a nitrogen stream. The crystalline material was removed by filtration and vacuum dried to yield 60 mg of product. It should be noted, however, that this preparation was contaminated with approximately 25% of the nonoxidized (TPP)Fe(ClO<sub>4</sub>) complex.

**(OEP)FeCl(ClO<sub>4</sub>).** Iron(III) octaethylporphyrin chloride (100 mg) was dissolved in methylene chloride (100 mL) which was 0.1 M in Bu<sub>4</sub>NClO<sub>4</sub>. Oxidation at 1.05 V for 20 min was accompanied by a current drop from 70 to 1 mA. The solution volume was reduced by rotary evaporation. When ~5 mL of solution remained, 10 mL of acetone was bled into the evaporation flask, and rotary evaporation was continued until the volume was reduced to 5 mL. The solid product was separated by filtration, washed with 2 mL of acetone, and vacuum dried for 4 h at room temperature. A 92-mg yield of (OEP)FeCl(ClO<sub>4</sub>) was obtained.

**Instrumentation.** Electrochemical measurements and preparations were carried out with a Princeton Applied Research Model (PAR) 173D potentiostat coupled with the Model 175 universal programmer and Model 176D digital coulometer. A conventional three-electrode system was employed. Cyclic voltammetric potentials were recorded vs. a Ag|AgNO<sub>3</sub> (0.01 M) in acetonitrile electrode, with platinum working (bead) and auxiliary (wire) electrodes. Reported potentials are corrected to the SCE electrode (PAR) by using an experimentally measured conversion factor of 0.33 V (potentials vs. SCE are 0.33 V more positive). For preparation scale electrolysis as described above, arbitrary potentials were measured vs. a silver wire immersed in the supporting electrolyte solution (separated from the bulk solution).

Nuclear magnetic resonance spectra were recorded in the pulsed Fourier transform mode on Bruker HX-90E and multinuclear JEOL FX 90 Q spectrometers. Chemical shifts are reported with respect to internal Me<sub>4</sub>Si, and downfield shifts are given positive sign. Temperature calibration was by the Van Geet methanol or ethylene glycol thermometers.<sup>27</sup>

Solution magnetic moment determinations were based on the NMR bulk susceptibility technique reported by Evans.<sup>28</sup> Solvent density corrections for variable-temperature work were taken into account, although in the absence of data for methylene chloride the temperature dependence for chloroform was utilized.<sup>29</sup> Diamagnetic corrections were taken from a recent report by Eaton and Eaton.<sup>30</sup> Solid-state measurements were made by using a Cahn Model 7600 Faraday system.

Infrared spectra were recorded on a Beckman Model IR-20A instrument using a scan rate of 81 cm<sup>-1</sup>/min. Samples were prepared as Nujol mulls and the thick paste was smeared onto a single sodium chloride plate. Although KBr pellets were made initially, bromide ion was found to reduce the oxidized complex. Integrity of the mull samples was verified by NMR after the infrared spectrum was recorded (the Nujol was removed with a heptane wash prior to sample dissolution in CD<sub>2</sub>Cl<sub>2</sub> and proton NMR examination).

Visible-ultraviolet absorption spectra were recorded on Cary 118 and Cary 219 spectrophotometers. Electron spin resonance spectra were

Table I. Half-Wave Potentials for Cyclic Voltammetric Oxidation of Iron(III) Porphyrins<sup>a</sup>

| monomers                              | first oxidatn | dimers   | first oxidatn | second oxidatn |
|---------------------------------------|---------------|--|---------------|----------------|
| (TPP)FeCl <sup>b</sup>                | 1.11          | [(TPP)Fe] <sub>2</sub> O <sup>b</sup>                | 0.83          | 1.09           |
| TPP( <i>p</i> -OCH <sub>3</sub> )FeCl | 1.02          | {TPP( <i>p</i> -OCH <sub>3</sub> )Fe} <sub>2</sub> O | 0.71          | 0.89           |
| (OEP)FeCl <sup>b</sup>                | 1.01          | [(OEP)Fe] <sub>2</sub> O <sup>b</sup>                | 0.67          | 0.98           |
| (ETIO)FeCl                            | 1.00          | [(ETIO)Fe] <sub>2</sub> O                            | 0.66          | 0.97           |

<sup>a</sup> Potentials taken as the midpoint of reversible anodic and cathodic waves, referenced to SCE, CH<sub>2</sub>Cl<sub>2</sub> solvent, Bu<sub>4</sub>NClO<sub>4</sub> 0.1 M, iron porphyrin 0.002 M, 25 °C, uncertainties ±0.02 V. <sup>b</sup> Equivalent to values reported in refs 13 and 14.

obtained with a Varian Model V-4502 X-band spectrometer. Solutions approximately 2 mM in methylene chloride-toluene (1:1) were examined at 77 K.

Mössbauer spectra for oxidized crystalline products were kindly provided by Professor D. N. Hendrickson of the University of Illinois.

## Results

**Electrochemical Oxidations.** Electrochemical generation of oxidized metalloporphyrins in nonaqueous media is straightforward and has been reported for several species.<sup>10,12-14,31-35</sup> However, isolation of the reactive product presents a formidable challenge due to the large excess (up to 100 times) of supporting electrolyte. Felton et al. employed a boiling water wash to remove Pr<sub>4</sub>NClO<sub>4</sub> from oxidized iron porphyrin products in the solid residue obtained from evaporation of the electrolysis mixture.<sup>13</sup> In our hands this washing procedure served to reduce a large part of the product to the parent iron(III) species. Accordingly, separation methods described here were devised on the basis of selective solubility of iron porphyrins and supporting electrolytes in various organic solvents. Unfortunately, the differing solubilities and reactivities of diverse iron porphyrin structural types have at this time precluded a general separation scheme.

Addition of electron-releasing substituents to the porphyrin ring is known to lower the oxidation potential<sup>36</sup> and should likewise stabilize higher oxidation states. In this regard the *p*-methoxyphenyl-substituted TPP proved to be more attractive than the unsubstituted compound. Likewise, porphyrins with alkylpyrrole substituents were much easier to oxidize.<sup>20</sup> Oxidation potentials with respect to the SCE are summarized in Table I for the compounds utilized in this study.

Control of oxidation potential through variation of axial ligand was also attempted. Surprisingly, however, the oxidation potentials for (TPP)Fe<sup>III</sup> complexed with 12 different anions were essentially invariant at 1.08–1.11 V.<sup>20</sup>

Reversibility of oxidations was demonstrated by several means. Cyclic voltammetric waves for isolated oxidized products were identical with those for the parent iron(III) compounds, with the exception of a slightly enhanced intensity for the cathodic wave corresponding to Fe(oxidized) ⇌ Fe(II). This behavior is expected for a solution in which the bulk species is in the oxidized state.

Reduction of oxidized compounds in methylene chloride using Bu<sub>4</sub>NI also served to demonstrate that the macrocycle had not been irreversibly modified. Thin-layer chromatography revealed >95% of recovered material was the parent iron(III) porphyrin. Visible-ultraviolet and NMR spectroscopy were also consistent with regeneration of the parent iron(III) porphyrin as discussed below.

**Chemical Oxidation.** Chemical oxidation of iron(III) porphyrins by an oxidized iron porphyrin of higher potential provides a ready

(31) Dolphin, D.; Forman, A.; Borg, D. C.; Fajer, J.; Felton, R. H. *Proc. Natl. Acad. Sci. U.S.A.* **1971**, *68*, 614–618.

(32) Fajer, J.; Borg, D. C.; Forman, A.; Felton, R. H.; Vegh, L.; Dolphin, D. *Ann. N. Y. Acad. Sci.* **1973**, *206*, 349–364.

(33) Spaulding, L. D.; Eller, P. G.; Bertrand, J. A.; Felton, R. H. *J. Am. Chem. Soc.* **1974**, *96*, 982–987.

(34) Fajer, J.; Borg, D. C.; Forman, A.; Adler, A. D.; Varadi, V. *J. Am. Chem. Soc.* **1974**, *96*, 1238–1239.

(35) Fuhrop, J.-H. *Struct. Bonding* (Berlin) **1974**, *18*, 1–67.

(36) Kadish, K. M.; Morrison, M. M.; Constant, L. A.; Dickens, L.; Davis, D. G. *J. Am. Chem. Soc.* **1976**, *98*, 8387–8390.

(27) Van Geet, A. L. *Anal. Chem.* **1968**, *40*, 2227–2229.

(28) Evans, D. F. *J. Chem. Soc.* **1959**, 2003–2005.

(29) "International Critical Tables"; Washburn, E. W., Ed.; McGraw-Hill: New York, 1928; Vol. 3, p 27.

(30) Eaton, S. S.; Eaton, G. R. *Inorg. Chem.* **1980**, *19*, 1095–1096.

Table II. Mössbauer Spectroscopy of Oxidized Iron Porphyrin Species

| compd  | T, K | IS, <sup>a</sup> mm/s | QS, mm/s | Γ <sub>-</sub> <sup>b</sup> | Γ <sub>+</sub> <sup>b</sup> | ref |
|--|------|-----------------------|----------|-----------------------------|-----------------------------|-----|
| {TPP( <i>p</i> -OCH <sub>3</sub> )Fe} <sub>2</sub> O                                 | 298  | 0.34                  | 0.59     | 0.39                        |                             | 45  |
|  | 78   | 0.42                  | 0.63     | 0.36                        |                             | 45  |
| {TPP( <i>p</i> -OCH <sub>3</sub> )Fe} <sub>2</sub> O(ClO <sub>4</sub> )              | 298  | 0.28                  | 0.50     | 0.42                        | 0.46                        | c   |
|  | 77   | 0.38                  | 0.57     | 0.54                        | 0.53                        | c   |
| {TPP( <i>p</i> -OCH <sub>3</sub> )Fe} <sub>2</sub> O(ClO <sub>4</sub> ) <sub>2</sub> | 77   | 0.38                  | 0.51     | 0.28                        | 0.29                        | c   |
| TPP( <i>p</i> -OCH <sub>3</sub> )FeCl  | 4    | 0.38                  | 1.03     | 0.81                        |                             | 46  |
| TPP( <i>p</i> -OCH <sub>3</sub> )FeCl(ClO <sub>4</sub> )                             | 77   | 0.41                  | 0.69     | 0.28                        | 0.34                        | c   |
| (TPP)FeCl  | 4    | 0.42                  | 0.46     | 0.29                        | 0.42                        | 47  |
| (TPP)Fe(ClO <sub>4</sub> )   | 295  | 0.29                  | 2.79     | 0.25                        | 0.26                        | 48  |
|  | 4    | 0.39                  | 3.5      | 0.39                        | 0.33                        | 48  |
| (TPP)FeCl(ClO <sub>4</sub> ) 22%   | 77   | 0.41                  | 3.26     |                             |                             | c   |
| 78%  | 77   | 0.45                  | 1.27     |                             |                             | c   |
| (TPP)FeCl(SbCl <sub>6</sub> )  | 77   | 0.40                  | 0.55     | 0.32                        | 0.35                        | 21  |
| (TPP)FeCl + <i>m</i> -chloroperoxybenzoic acid                                       | ?    | 0.05                  | 1.49     |                             |                             | 15b |
| (TPP)FeCl + iodosylbenzene   | ?    | -0.03                 | 2.13     |                             |                             | 15b |
| HRP (resting)  | 77   | 0.25                  | 1.96     |                             |                             | 4a  |
| HRP compound II  | 77   | 0.03                  | 1.36     |                             |                             | 4a  |
| HRP compound I   | 77   | 0.00                  | 1.20     |                             |                             | 4a  |

<sup>a</sup> Isomer shift with respect to metallic iron. <sup>b</sup> Line width in mm/s at half-height. <sup>c</sup> This work.

means of generating solution species which might otherwise be isolated from supporting electrolyte with difficulty. This method of in situ oxidation has been demonstrated previously for preparation of oxidized natural-derivative iron porphyrins using [(TPP)Fe]<sub>2</sub>O(ClO<sub>4</sub>)<sub>2</sub><sup>37</sup> and also for generation of zinc  $\pi$ -cation radical porphyrins using [(TPP)Fe]<sub>2</sub>O(ClO<sub>4</sub>)<sub>2</sub>.<sup>34</sup>

An additional chemical oxidation method is possible for iron porphyrins with relatively low oxidation potentials. Thus, an iodine-silver perchlorate oxidizing agent has previously been utilized for generation of zinc porphyrin  $\pi$ -cation radical species.<sup>38</sup> In practice a small stoichiometric excess (10%) of standard iodine-methylene chloride solution is added to the iron porphyrin dissolved in methylene chloride. Titration with an equivalent of silver perchlorate-acetone solution effects one-electron oxidation of ( $\mu$ -oxo)iron(III) dimers (with partial cleavage of dimer) and iron octaethylporphyrin or etioporphyrin perchlorate ((ETIO)-FeClO<sub>4</sub>) complexes. Precipitated silver iodide is removed by centrifuge. These in situ oxidations yield products identical with those prepared by electrochemical oxidation, as verified by NMR and visible-ultraviolet spectroscopy. It should be noted that neither iodine nor silver ion alone will oxidized iron(III) porphyrins under conditions noted above.

Attempted air oxidation of ( $\mu$ -oxo)iron(III) dimers in the presence of strong Lewis acids (BF<sub>3</sub>, Et<sub>2</sub>O·BF<sub>3</sub>, HBF<sub>4</sub>, HPF<sub>6</sub>) did not yield species spectroscopically resembling electrochemically oxidized materials.<sup>39,40</sup>

**Elemental Analysis.** Elemental analysis helped verify formulations of the oxidized compounds as perchlorate salts. For example, total chloride analysis (Galbraith Laboratories) of [(TPP)Fe]<sub>2</sub>O(ClO<sub>4</sub>)(C<sub>7</sub>H<sub>8</sub>) and [FeTPP]<sub>2</sub>O(ClO<sub>4</sub>)<sub>2</sub> yielded values of 2.94% and 4.60%, to be compared with theoretical values of 2.30% and 4.57%, respectively. Iron analysis by a modified *o*-phenanthroline method<sup>41</sup> was used as a basis for magnetic susceptibility and molar absorptivity calculations. Results demonstrated the near analytical purity of oxidized products, as for example in the case of [(TPP)Fe]<sub>2</sub>O(ClO<sub>4</sub>)(C<sub>7</sub>H<sub>8</sub>): 7.10% experimental; 7.23% theoretical. Carbon, hydrogen, and nitrogen analyses were not consistently satisfactory, although deviations (generally low values of 0.3–1.0% absolute) were no larger than

those frequently observed for iron(III) compounds. Retention of trace, nonstoichiometric amounts of solvent or supporting electrolyte may explain the poor analyses. Identification of such contaminants was generally possible in NMR spectra.

**Infrared Spectroscopy.** Infrared spectral examination of oxidized  $\mu$ -oxo dimeric species served to confirm integrity of the oxo linkage. Bands near 870 and 890 cm<sup>-1</sup> have been assigned to the asymmetric Fe–O–Fe stretch in [(TPP)Fe]<sub>2</sub>O.<sup>42,43</sup> These bands are observed with some intensity changes for corresponding single- and double-electron oxidation products prepared as Nujol mulls.<sup>44</sup> A strong, broad band at ~1100 cm<sup>-1</sup> in the oxidized dimers results from the perchlorate anion. Comparison with spectra of (TPP)Fe(ClO<sub>4</sub>) and (TPP)Zn(ClO<sub>4</sub>) (for which perchlorate coordination has been demonstrated<sup>33</sup>) suggests that perchlorate ion is not coordinated in the solid state. The ~1100-cm<sup>-1</sup> band is also observed for methylene chloride solutions of [(TPP)Fe]<sub>2</sub>O(ClO<sub>4</sub>)<sub>2</sub> and (OEP)FeCl(ClO<sub>4</sub>).

An additional feature of the IR spectra is found in the appearance of a new, very intense band in the 1280-cm<sup>-1</sup> region for oxidized TPPFe derivatives as well as for the  $\pi$ -cation radical (TPP)Zn(ClO<sub>4</sub>).<sup>44</sup> This band thus appears to be associated with porphyrin-centered (vs. metal-centered) oxidation. The 1280-cm<sup>-1</sup> band is absent in (OEP)FeCl(ClO<sub>4</sub>), but a new, strong band appears near 1550 cm<sup>-1</sup>.

**Magnetic Measurements.** Solution magnetic measurements were performed by the NMR (Evans's) method<sup>28</sup> by using Me<sub>4</sub>Si as the reference substance. Simultaneous recording of the complete proton NMR spectra served to demonstrate integrity of compounds. Calculations are based on the iron content of the derivative. Dimeric ( $\mu$ -oxo)iron porphyrins exhibit low moments as a consequence of metal-metal antiferromagnetic coupling. Thus, the solid-state magnetic moment for [(TPP)Fe]<sub>2</sub>O is 2.5  $\mu_B$  per dimeric unit at room temperature.<sup>42</sup> For the oxidized product [(TPP)Fe]<sub>2</sub>O(ClO<sub>4</sub>) effective moments per dimeric unit in methylene chloride solvent were 3.2  $\pm$  0.2 and 3.1  $\pm$  0.2  $\mu_B$  at 299 and 270 K, respectively. The doubly oxidized dimer [TPP(*p*-OCH<sub>3</sub>)Fe]<sub>2</sub>O(ClO<sub>4</sub>)<sub>2</sub> exhibited an even lower moment of 1.7  $\pm$  0.1  $\mu_B$  per dimer unit at 280 K. Poor solubility precluded measurements at lower temperature. Observed values for [(TPP)Fe]<sub>2</sub>O(ClO<sub>4</sub>) are consistent with the previously reported 2.9  $\mu_B$  magnetic moment at 313 K.<sup>14</sup>

(37) Phillippi, M. A.; Goff, H. M. *J. Am. Chem. Soc.* **1979**, *101*, 7641–7643.

(38) Shine, H. J.; Padilla, A. G.; Wu, S.-M. *J. Org. Chem.* **1979**, *44*, 4069–4075.

(39) Wollmann, R. G.; Hendrickson, D. N. *Inorg. Chem.* **1977**, *16*, 723–733.

(40) Cohen, I. A.; Lavallee, D. K.; Kopelove, A. B. *Inorg. Chem.* **1980**, *19*, 1098–1100.

(41) (a) Willard, H. H.; Merritt, L. L.; Dean, J. A. "Instrumental Methods of Analysis" 5th ed.; Van Nostrand: New York, 1974; p 113. (b) Phillippi, M. A. Ph.D. Dissertation, University of Iowa, 1980.

(42) Cohen, I. A. *J. Am. Chem. Soc.* **1969**, *91*, 1980–1983.

(43) Fleischer, E. B.; Srivastava, T. S. *J. Am. Chem. Soc.* **1969**, *91*, 2403–2405.

(44) Shimomura, E. T.; Phillippi, M. A.; Goff, H. M.; Scholz, W. F.; Reed, C. A. *J. Am. Chem. Soc.* **1981**, *103*, 6778–6780.

(45) Torrens, M. A.; Straub, D. K.; Epstein, L. M. *J. Am. Chem. Soc.* **1972**, *94*, 4160–4162.

(46) Torrens, M. A.; Straub, D. K.; Epstein, L. M. *J. Am. Chem. Soc.* **1972**, *94*, 4162–4167.

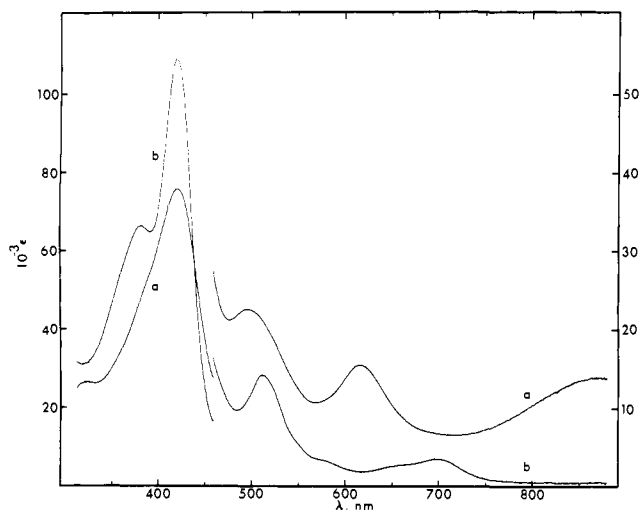


**Figure 1.** Electronic absorption spectra of (a) TPP(*p*-OCH<sub>3</sub>)FeCl(ClO<sub>4</sub>) (CH<sub>2</sub>Cl<sub>2</sub> solvent) and (b) product from reduction by Bu<sub>4</sub>NI.

Monomeric oxidized iron porphyrins exhibit magnetic moments which are slightly lower than the 5.9- $\mu_B$  value of the parent high-spin iron(III) compounds. An unusual moment of  $5.5 \pm 0.1 \mu_B$  is observed for both TPP(*p*-OCH<sub>3</sub>)FeCl(ClO<sub>4</sub>) and for (OEP)FeCl(ClO<sub>4</sub>) in methylene chloride, over temperature ranges of 218–299 and 248–293 K, respectively. A room-temperature solid-state measurement of TPP(*p*-OCH<sub>3</sub>)FeCl(ClO<sub>4</sub>) by the Faraday method yielded an equivalent moment of  $5.4 \mu_B$ . A value of  $4.9 \mu_B$  previously reported from this laboratory for TPP(*p*-OCH<sub>3</sub>)FeCl(ClO<sub>4</sub>) is low as a consequence of assuming analytical purity of the product rather than using the measured iron content.<sup>37</sup> Values of  $5.1$  and  $4.9 \mu_B$  for (TPP)FeCl(ClO<sub>4</sub>) and (OEP)-FeCl(ClO<sub>4</sub>) were reported by Felton et al.<sup>14</sup> The recently prepared (TPP)FeCl(SbCl<sub>6</sub>) complex exhibits a solid-state  $\mu_{\text{eff}} = 5.1 \mu_B$  value over the temperature range 5–300 K.<sup>21</sup>

Electron spin resonance measurements of [(TPP)Fe]<sub>2</sub>O(ClO<sub>4</sub>) at 77 K in 1:1 methylene chloride-toluene revealed a sharp ( $\Delta w_{1/2} \approx 30$  G)  $g \approx 2.0$  signal, as noted previously.<sup>14</sup> Examination of the doubly oxidized dimer and singly oxidized monomeric compounds under the same experimental conditions yielded only trace  $g = 6$  signals from high-spin iron(III) impurities.

**Mössbauer Spectroscopy.** Table II summarizes results of Mössbauer experiments with oxidized iron porphyrins. Literature parameters for parent iron(III) derivatives and other relevant species are also included. Oxidized dimeric compounds show a small but significant decrease in isomer shift values when compared with parent iron(III) dimers. Subtle changes are also apparent in quadrupole splittings and line widths. Unlike parent iron(III) complexes, the oxidized monomeric species yield sharp signals at 77 K. Quadrupole splitting values are both increased and decreased depending on TPP substituents. Isomer shift values are surprisingly slightly increased for oxidized monomeric derivatives. Decreased isomer shifts are expected for an iron(IV) complex. This is apparent for the oxidized states of HRP listed in Table II, for *m*-chloroperoxybenzoic acid and iodosylbenzene-oxidized TPP(2,4,6-CH<sub>3</sub>)FeCl.<sup>15b</sup> and for various other inorganic complexes formulated as iron(IV) species.<sup>49–52</sup>

**Electronic Spectra.** Visible-ultraviolet spectroscopy provides a ready means of monitoring electrochemical oxidations and reductive titrations of isolated products. With respect to the parent

**Table III.** Electronic Absorption Spectra of Iron Porphyrins<sup>a</sup>

| compd   | wavelength maxima, nm (molar absorptivity, $\times 10^{-3} \text{ m}^{-1} \text{ cm}^{-1}$ )   |
|---|--|
| (TPP)FeCl <sup>b</sup>  | 380 sh (59.0), 417 (110), 511 (13.4), 577 sh (3.3), 658 sh (2.8), 690 (3.2)                    |
| (TPP)FeCl(ClO <sub>4</sub> )  | 397 (65), <sup>c</sup> 530 (15), <sup>c</sup> 600 sh (10), <sup>c</sup> 820 (5.0) <sup>d</sup> |
| (TPP)( <i>p</i> -OCH <sub>3</sub> )FeCl <sup>d</sup>  | 385 sh (58.6), 421 (109), 512 (13.7), 575 sh (3.2), 605 sh (2.4), 660 sh (2.6), 700 (3.4)      |
| TPP( <i>p</i> -OCH <sub>3</sub> )FeCl(ClO <sub>4</sub> ) <sup>d</sup>                             | 324 sh (26), 421 (76), 496 (23), 615 (15.5), 870 (14)  |
| [(TPP)Fe] <sub>2</sub> O <sup>e</sup>   | 408 (106), 571 (10.7), 612 (4.8)   |
| [(TPP)Fe] <sub>2</sub> O(ClO <sub>4</sub> ) <sup>d</sup>  | 405 (94.6), 570 (7.0) (very broad long wavelength bands)                                       |
| [(TPP)Fe] <sub>2</sub> O(ClO <sub>4</sub> ) <sub>2</sub> <sup>d</sup>                             | 397 (67), 450 sh (45), 550 (21)  |
| [TPP( <i>p</i> -OCH <sub>3</sub> )Fe] <sub>2</sub> O <sup>d</sup>                                 | 411 (107), 575 (8.1), 615 (5.8)  |
| [TPP( <i>p</i> -OCH <sub>3</sub> )Fe] <sub>2</sub> O(ClO <sub>4</sub> ) <sup>d</sup>              | 416 (100), 525 (9.2), 625 (8.1), 830 (4.4)   |
| [TPP( <i>p</i> -OCH <sub>3</sub> )Fe] <sub>2</sub> O(ClO <sub>4</sub> ) <sub>2</sub> <sup>d</sup> | 414 (69), 565 (13.3), 630 (13.4), 855 (10)   |
| (OEP)FeCl <sup>d</sup>  | 378 (99.6), 504 (8.7), 534 (9.0), 578 (2.6), 634 (4.5)   |
| (OEP)FeCl(ClO <sub>4</sub> ) <sup>d</sup>   | 356 (80), 519 (7.7), 574 (4.4), 610 (3.3), 630 (3.0) (very broad long wavelength bands)        |
| [(OEP)Fe] <sub>2</sub> O <sup>d</sup>   | 342 sh (42), 384 (62), 558 (6.8), 594 (5.8)  |
| [(OEP)Fe] <sub>2</sub> O(ClO <sub>4</sub> ) <sup>c</sup>  | 375 (52), 570 (5)  |

<sup>a</sup> Unless otherwise noted, CH<sub>2</sub>Cl<sub>2</sub> solvent, 25 °C, iron porphyrin  $1 \times 10^{-5}$  to  $2 \times 10^{-4}$  M. Molar absorptivity for dimers is per iron atom. <sup>b</sup> Reference 53. <sup>c</sup> Values taken from spectra in ref 14; confirmed in this study. <sup>d</sup> This work. <sup>e</sup> Reference 53, C<sub>6</sub>H<sub>6</sub> solvent.

iron(III) compounds, generalizations can be made for oxidized species concerning the appearance of a Soret band of diminished intensity and increased absorption in the long wavelength region. In an earlier study, Felton et al.<sup>13,14</sup> noted blue-shifted Soret bands and broad, featureless visible region absorptions for oxidized (TPP)FeCl and (OEP)FeCl complexes. However, the spectrum of TPP(*p*-OCH<sub>3</sub>)FeCl(ClO<sub>4</sub>) in Figure 1 serves to demonstrate that the Soret band is not necessarily blue-shifted upon oxidation (corresponding oxidized dimers actually show red-shifted Soret bands), and well-defined visible region bands may result. Another distinctive feature of this spectrum is the appearance of a broad absorption in the 870-nm region. Although isoporphyrins (ring modified species) are known to give such long wavelength absorptions, the reversibility upon iodide reduction appears to demonstrate association of this band with the  $\pi$ -cation radical. Despite the spectral differences between (TPP)FeCl(ClO<sub>4</sub>) and TPP(*p*-OCH<sub>3</sub>)FeCl(ClO<sub>4</sub>), the electronic structures are equivalent as judged by NMR spectra. Visible-ultraviolet spectral parameters listed in Table III are generally in agreement with earlier published spectra.<sup>12–14</sup>

**NMR Spectra of  $\mu$ -Oxo Dimers.** Proton NMR spectra have been reported for the singly<sup>13,14,37</sup> and doubly oxidized<sup>37</sup>  $\mu$ -oxo dimeric iron porphyrins. Small isotropic shifts reflect the weak paramagnetic character as a consequence of antiferromagnetic coupling through the oxo bridge. Resonances for various TPP derivatives are listed in Table IV. Difficulties with separation of supporting electrolyte from ortho- and meta-methyl-substituted TPP species demanded an alternate preparative route. Accordingly, these compounds were oxidized in situ by using the silver perchlorate-iodine method. The utility of this oxidant for single-electron oxidation of [(TPP)Fe]<sub>2</sub>O and [(TPP)(*p*-OCH<sub>3</sub>)Fe]<sub>2</sub>O was also verified. Changes in signal intensity among ortho-, meta-, and para-substituted TPP species thus permitted the assignments for singly oxidized dimers listed in Table IV. Upon titration with the parent iron(III) dimer or with a reducing agent such as Bu<sub>4</sub>NI,

(47) Maricondi, C.; Straub, D. K.; Epstein, L. M. *J. Am. Chem. Soc.* **1972**, *94*, 4157–4159.

(48) Spartalian, K.; Lang, G.; Reed, C. A. *J. Chem. Phys.* **1979**, *71*, 1832–1837.

(49) Pasek, E. A.; Straub, D. K. *Inorg. Chem.* **1972**, *11*, 259–263.

(50) Paez, E. A.; Weaver, D. L.; Oosterhuis, W. T. *J. Chem. Phys.* **1972**, *57*, 3709–3715.

(51) Petridis, D.; Niarchos, D.; Kanellakopoulos, B. *Inorg. Chem.* **1979**, *18*, 505–509.

(52) Coucouvanis, D. "Progress in Inorganic Chemistry"; Lippard, S. J., Ed.; Wiley: New York, 1979; Vol. 26, pp 301–469.

(53) Fleischer, E. B.; Palmer, J. M.; Srivastava, T. S.; Chatterjee, A. *J. Am. Chem. Soc.* **1971**, *93*, 3162–3167.

Table IV. Proton NMR Spectra of ( $\mu$ -Oxo)iron Porphyrin Dimers<sup>a</sup>

| compd  | pyr-<br>role | ortho    | meta | para     | CH <sub>3</sub> |
|--|--------------|----------|------|----------|-----------------|
| [(TPP)Fe] <sub>2</sub> O   | 13.4         | 7.6      | 7.6  | 7.6      |                 |
| [(TPP)Fe] <sub>2</sub> O(ClO <sub>4</sub> )  | 12.3         | 1.3      | 11.7 | 3.2      |                 |
| [(TPP)Fe] <sub>2</sub> O(ClO <sub>4</sub> ) <sub>2</sub>                             | 9.7          | 4.3      | 8.8  | <i>b</i> |                 |
| [TPP( <i>p</i> -OCH <sub>3</sub> )Fe] <sub>2</sub> O                                 | 13.4         | 7.2      | 7.2  |          | 4.16            |
| [TPP( <i>p</i> -OCH <sub>3</sub> )Fe] <sub>2</sub> O(ClO <sub>4</sub> )              | 13.0         | 1.3      | 10.6 |          | 5.3             |
| [TPP( <i>p</i> -OCH <sub>3</sub> )Fe] <sub>2</sub> O(ClO <sub>4</sub> ) <sub>2</sub> | 10.1         | 3.6      | 7.7  |          | 4.35            |
| [TPP( <i>m</i> -CH <sub>3</sub> )Fe] <sub>2</sub> O                                  | 13.4         | 7.4      | 7.4  | 7.4      | 2.59,<br>2.46   |
| [TPP( <i>m</i> -CH <sub>3</sub> )Fe] <sub>2</sub> O(ClO <sub>4</sub> ) <sup>c</sup>  | 12.2         | <i>d</i> | 11.6 | 3.0      | 1.32,<br>1.07   |
| [TPP( <i>o</i> -CH <sub>3</sub> )Fe] <sub>2</sub> O                                  | 13.7         | 7.6      | 7.6  | 7.6      | 1.46            |
| [TPP( <i>o</i> -CH <sub>3</sub> )Fe] <sub>2</sub> O(ClO <sub>4</sub> ) <sup>c</sup>  | 12.0         | <i>d</i> | 11.6 | 5.7      | 3.9             |

| compd   | ethyl-<br>CH <sub>2</sub> | ethyl-<br>CH <sub>3</sub> | ring-<br>CH <sub>3</sub> | meso                 |
|---|---------------------------|---------------------------|--------------------------|----------------------|
| [(OEP)Fe] <sub>2</sub> O                                  | 6.04, 5.08                | 1.75                      |                          | (~5.5 <sup>e</sup> ) |
| [(OEP)Fe] <sub>2</sub> O(ClO <sub>4</sub> )               | 16.1, 13.1                | 2.6                       |                          | -0.8                 |
| [(ETIO)Fe] <sub>2</sub> O                                 | 6.09, 5.16                | 1.82                      | 5.16                     | <i>f</i>             |
| [(ETIO)Fe] <sub>2</sub> O(ClO <sub>4</sub> ) <sup>c</sup> | 14.7, 14.0                | 2.5                       | 28.0                     | <i>f</i>             |

<sup>a</sup> Iron porphyrins 3–10 mM in CD<sub>2</sub>Cl<sub>2</sub> or CDCl<sub>3</sub>, 26 °C, Me<sub>4</sub>Si reference. <sup>b</sup> Under solvent. <sup>c</sup> Prepared by AgClO<sub>4</sub>/I<sub>2</sub> oxidation; others prepared by electrochemical oxidation. <sup>d</sup> Signal under methyl resonances. <sup>e</sup> Not observed due to overlap, value from ref 57. <sup>f</sup> Signal not observed due to low solubility.

the resonances assigned to phenyl protons migrated (averaged signals in the fast-exchange limit were observed) to the 7.6-ppm region of the parent dimer and the pyrrole proton signal moved to 13.4 ppm.<sup>37</sup>

Resonances for electrochemically generated, doubly oxidized dimers were similarly assigned by titration with the parent iron(III) dimer. Rapid intra and intermolecular electron exchange yields averaged signals which match those for the singly oxidized dimer with 1:1 mixing of for example [(TPP)Fe]<sub>2</sub>O and [(TPP)Fe]<sub>2</sub>O(ClO<sub>4</sub>)<sub>2</sub>.<sup>37</sup>

Oxidation of [(OEP)Fe]<sub>2</sub>O at the first cyclic voltammetric wave yielded the one-electron oxidation product [(OEP)Fe]<sub>2</sub>O(ClO<sub>4</sub>) as well as ~30% of a previously unidentified complex.<sup>54</sup> Resonances of the oxidized dimer were readily assigned by titration of [(OEP)Fe]<sub>2</sub>O(ClO<sub>4</sub>) with the parent iron(III) dimer. Impurity resonances remained stationary during the titration, whereas signals for the  $\mu$ -oxo dimer shifted as the mole-weighted average of oxidized and iron(III) resonances. The oxidized (ETIO)Fe dimer was generated in situ by silver perchlorate-iodine oxidation. Assignments (Table IV) follow from and confirm those for [(OEP)Fe]<sub>2</sub>O(ClO<sub>4</sub>). Successful isolation of the doubly oxidized [(OEP)Fe]<sub>2</sub>O complex has not yet been realized.

Partial carbon-13 NMR spectra of oxidized dimers have also been recorded in spite of low solubilities, line broadening, and possible decomposition of sample during long spectral accumulations. Assignments were made by selective frequency decoupling experiments and shift of signals with partial reduction of the oxidized complex.<sup>55,56</sup> At 299 K with use of CD<sub>2</sub>Cl<sub>2</sub> solvent the following signals are observed for [(TPP)Fe]<sub>2</sub>O(ClO<sub>4</sub>): ortho-C, 304 ppm;  $\beta$ -pyrrole-C, 240 ppm; para-C, 150.6 ppm; meta-C, 130.9, 129.5 ppm.

**NMR of Oxidized Monomeric Compounds.** Oxidized monomeric (TPP)Fe derivatives yield well-resolved proton NMR spectra which differ from parent iron(III) spectra most significantly in terms of much larger phenyl proton isotropic shifts. Proton NMR

(54) The iron(III) complex may be a di- $\mu$ -hydroxo dimer and is best generated by addition of water to a methylene chloride solution of (OEP)Fe(ClO<sub>4</sub>). Proton NMR resonances and assignments are as follows: CH<sub>2</sub>, 21.5, 19.6 ppm; CH<sub>3</sub>, 3.05 ppm; meso-H, -7.2 ppm. Variable-temperature measurements are consistent with antiferromagnetic coupling which is weaker than in the oxo dimer.

(55) Goff, H. *Biochim. Biophys. Acta* **1978**, *542*, 348–355.

(56) Phillippi, M. A.; Goff, H. M. *J. Chem. Soc., Chem. Commun.* **1980**, 455–456.

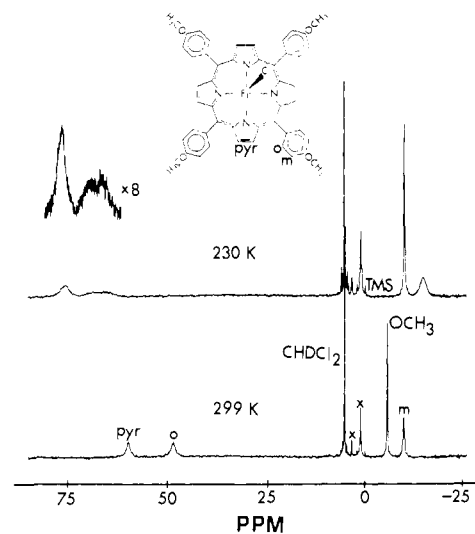


Figure 2. Proton NMR spectrum of TPP (*p*-OCH<sub>3</sub>)FeCl(ClO<sub>4</sub>) at 299 and 230 K (CD<sub>2</sub>Cl<sub>2</sub> solvent, Me<sub>4</sub>Si reference).

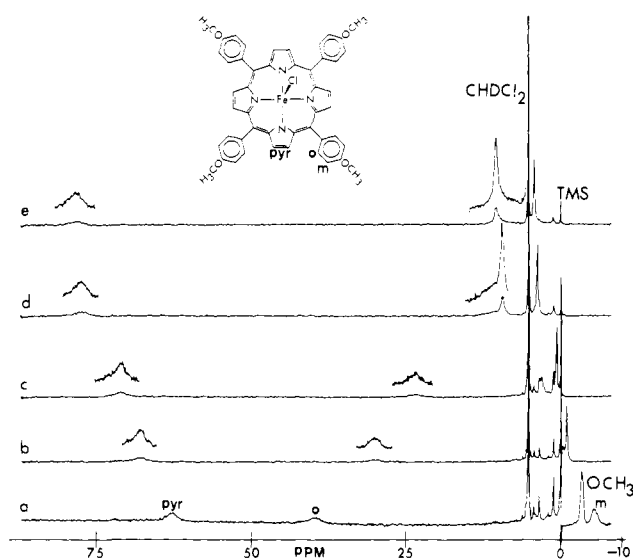


Figure 3. Proton NMR spectra of TPP (*p*-OCH<sub>3</sub>)FeCl(ClO<sub>4</sub>) with addition of TPP (*p*-OCH<sub>3</sub>)FeCl (CD<sub>2</sub>Cl<sub>2</sub> solvent, 26 °C). Mole fraction of TPP (*p*-OCH<sub>3</sub>)FeCl(ClO<sub>4</sub>): (a) 0.81; (b) 0.57; (c) 0.40; (d) 0.15; (e) 0.07.

spectra of TPP(*p*-OCH<sub>3</sub>)FeCl(ClO<sub>4</sub>) are shown in Figure 2 both at room temperature and at low temperature. Splitting of the ortho-phenyl proton resonance is apparent at 225 K, and the meta-proton signal splits at lower temperature. Such splitting is known for high-spin iron(III) derivatives and results from an iron atom out-of-plane configuration.<sup>57</sup> In this instance the splitting provides no resolution of the question of perchlorate binding, as lack of a center of symmetry in either a five-coordinate chloride complex or six-coordinate chloride-perchlorate complex could bring splitting of slowly rotating, orthogonal phenyl group resonances. It should be noted that ref 21 alludes to a preliminary X-ray structure of the oxidized (TPP)FeCl(SbCl<sub>6</sub>) in which SbCl<sub>6</sub><sup>-</sup> is not coordinated.

Figure 3 illustrates both a means of characterizing the oxidized monomeric complex and a useful technique for assigning resonances. Spectral effects of titrating the oxidized monomer with TPP(*p*-OCH<sub>3</sub>)FeCl are recorded in this series of spectra. Resonances represent the mole fraction weighted average of chemical shifts for the oxidized and parent compounds as noted previ-

(57) La Mar, G. N.; Walker, F. A. "The Porphyrins"; Dolphin, Ed.; Academic Press: New York, 1978; Vol. 4, pp 61–157.

Table V. Proton NMR Spectra of Monomeric Iron Porphyrins<sup>a</sup>

| compd   | pyrrole                    | ortho                      | meta          | para | CH <sub>3</sub>           |
|---|----------------------------|----------------------------|---------------|------|---------------------------|
| (TPP)FeCl   | 79.4                       | ~6                         | 13.3,<br>12.2 | 6.35 |                           |
| (TPP)FeCl(ClO <sub>4</sub> )  | 66.1                       | 37.6,<br>34.4              | -12.4         | 29.5 |                           |
| TPP( <i>p</i> -OCH <sub>3</sub> )FeCl                                 | 79.6                       | ~6                         | 12.8,<br>11.9 |      | 5.21                      |
| TPP( <i>p</i> -OCH <sub>3</sub> )FeCl(ClO <sub>4</sub> )              | 59.9<br>(170) <sup>b</sup> | 48.1<br>(277) <sup>b</sup> | -9.8          |      | -5.7<br>(57) <sup>b</sup> |
| TPP( <i>p</i> -OCH <sub>3</sub> )FeCl(ClO <sub>4</sub> ) <sup>c</sup> | 58.5                       | 47.3                       | -9.2          |      | -4.8                      |

| compd                                     | CH <sub>2</sub> | CH <sub>3</sub> | meso |
|---|-----------------|-----------------|------|
| (OEP)FeCl <sup>d</sup>                    | 43.1, 39.5      | 6.64            | -54  |
| (OEP)FeCl(ClO <sub>4</sub> ) <sup>e</sup> | 30.5, 29.6      | 3.16            | -18  |

<sup>a</sup> Except as noted oxidized species in CD<sub>2</sub>Cl<sub>2</sub> solvent, others in CDCl<sub>3</sub> solvent, iron porphyrin ~10 mM, 26 °C, Me<sub>4</sub>Si reference. <sup>b</sup> Line widths at half-height. <sup>c</sup> CD<sub>3</sub>CN solvent. <sup>d</sup> 30 °C. <sup>e</sup> 20 °C.

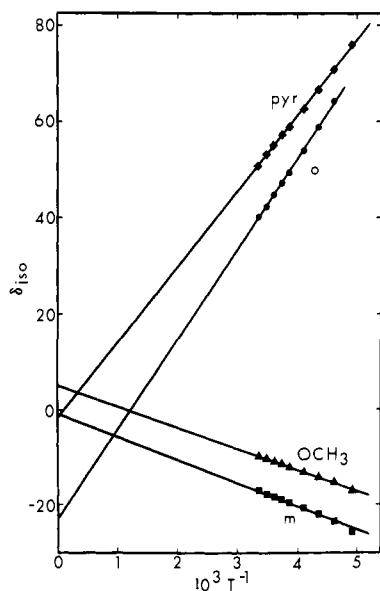


Figure 4. Curie law plots for TPP(*p*-OCH<sub>3</sub>)FeCl(ClO<sub>4</sub>) (CD<sub>2</sub>Cl<sub>2</sub> solvent).

ously.<sup>13,14</sup> This indicates that electron transfer is rapid on the NMR time scale, and most importantly that no porphyrin structural modification has occurred during electrochemical oxidation. Assignment of resonances follows from the limiting resonance positions observed when a large excess of TPP(*p*-OCH<sub>3</sub>)FeCl is present. The pyrrole resonance moves downfield upon titration, approaching the 79-ppm position where it is observed in the parent compound. Meta-H and para-OCH<sub>3</sub> signals progress downfield upon titration, whereas the ortho-H signal moves upfield. In parts d and e of Figure 3 the ortho- and meta-resonances actually cross as they move to ~7 and ~12 ppm, respectively. Titration of (TPP)FeCl(ClO<sub>4</sub>) with (TPP)FeCl yielded an equivalent result. In this latter oxidized species the para-H signal is nearly as far downfield at 29.5 ppm as that for the ortho-H (Table V). Examination of the oxidized meta-CH<sub>3</sub> derivative revealed, as expected, an upfield meta-H resonance matching the downfield para-H signal in intensity. Reductive titrations with Bu<sub>4</sub>Ni likewise served to quantitatively convert oxidized species to iron(III) porphyrins as monitored by proton NMR spectroscopy.

Extensive variable temperature results are summarized as Curie law plots in Figure 4. Plots are adequately linear and have nearly zero intercepts in the case of pyrrole and meta-H signals. Plots for ortho-H and para-OCH<sub>3</sub> resonances, on the other hand, exhibit sizeable upfield and downfield intercepts, respectively.

Spectra in Figure 5 illustrate effects of (OEP)FeCl oxidation to (OEP)FeCl(ClO<sub>4</sub>). Pyrrole methylene resonances in the parent

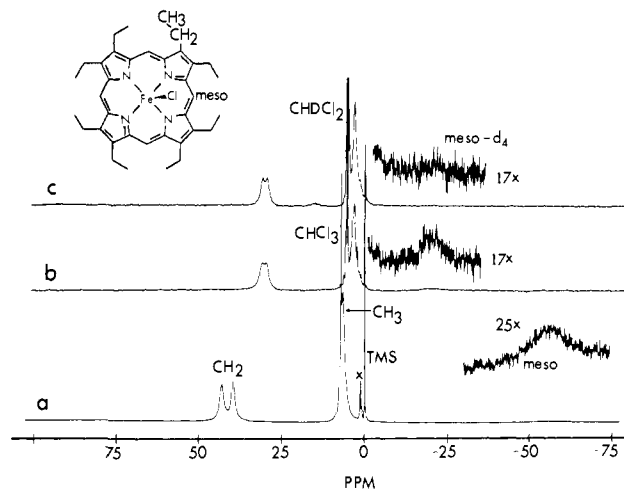


Figure 5. Proton NMR spectra of (OEP)FeCl and oxidized derivatives: (a) (OEP)FeCl, CDCl<sub>3</sub> solvent, 30 °C; (b) (OEP)FeCl(ClO<sub>4</sub>), CD<sub>2</sub>Cl<sub>2</sub> solvent, 20 °C; (c) meso-deuterated (OEP)FeCl(ClO<sub>4</sub>), CD<sub>2</sub>Cl<sub>2</sub> solvent, 20 °C.

iron(III) derivative are further downfield and show a larger splitting than is the case for the oxidized compound. Likewise, the upfield shift of the meso-H is attenuated in the oxidized state. The meso-H resonance at -18 ppm was assigned by deuteration as demonstrated in Figure 5c. This small meso-H shift is surprising when considering the large shifts for phenyl substituents in oxidized (TPP)Fe analogues. Structural integrity and redox reversibility of the oxidized material was demonstrated by titration with the parent iron(III) complex and with Bu<sub>4</sub>Ni, much as described for (TPP)Fe derivatives.

#### Discussion

Preparative scale electrochemical oxidations of iron(III) porphyrins have been reported by Wolberg and Manassen<sup>12</sup> and by Felton et al.<sup>13,14</sup> Wolberg and Manassen carried out oxidation of (TPP)FeOAc and other metalloporphyrins using benzonitrile-Bu<sub>4</sub>NClO<sub>4</sub> media. No isolation conditions were discussed, and it is assumed that magnetic and spectroscopic characterization of the product was performed on electrolyzed solutions. The singly oxidized product was identified as a low-spin iron(III) porphyrin  $\pi$ -cation radical on the basis of a magnetic moment value of 2.7  $\mu_B$ . This magnetic moment is considerably lower than values observed (in methylene chloride solvent) by Felton et al. (5.1  $\mu_B$ )<sup>14</sup> and reported here (5.5  $\mu_B$ ). Visible-ultraviolet spectra in all three cases appear to be equivalent. Benzonitrile coordination does not directly serve to explain the seemingly different spin states, as proton NMR spectra of TPP(*p*-OCH<sub>3</sub>)FeCl(ClO<sub>4</sub>) recorded in this study are equivalent for acetonitrile and methylene chloride solvents (Table V). A reasonable explanation may be based on supporting electrolyte displacement of an acetate ligand to yield the perchlorate adduct. This species is expected to exhibit a spin-admixed  $S = 5/2, 3/2$  electronic structure,<sup>48,58,59</sup> which in an oxidized radical form might be expected to exhibit a relatively low magnetic moment. In this regard it should be noted that Wolberg and Manassen report a 5.1- $\mu_B$  moment for the parent iron(III) porphyrin—a value considerably below the generally observed 5.9  $\mu_B$  spin-only value.

Felton et al.<sup>13,14</sup> have previously reported preparation of certain of the oxidized compounds described here. Visible-ultraviolet, ESR, electrochemical, and stability properties reported in the earlier study have for the most part been verified in this work. However, procedures for separation and isolation of products from supporting electrolyte have been extensively modified, as dissolution of electrolyte in boiling water seemingly reduces part of the oxidized product. Differences in NMR spectra discussed below

(58) Reed, C. A.; Mashiko, T.; Bentley, S. P.; Kastner, M. A.; Scheidt, W. R.; Spartalian, K.; Lang, G. *J. Am. Chem. Soc.* 1979, 101, 2948-2958.  
(59) Goff, H.; Shimomura, E. *J. Am. Chem. Soc.* 1980, 102, 31-37.

may be rationalized in part by presence of considerable iron(III) material and availability of less sophisticated NMR instrumentation at the time of the earlier study. Reassignment of phenyl proton NMR signals in [(TPP)Fe]<sub>2</sub>O(ClO<sub>4</sub>) has been reported from this laboratory.<sup>37</sup> Upfield shifts for ortho and para protons and a downfield shift for the meta-phenyl proton have been demonstrated through examination of oxidized ortho- and meta-methyl- and para-methoxy-substituted dimers. The magnitude of phenyl proton shifts in the oxidized monomeric (TPP)FeCl(ClO<sub>4</sub>) species is also appreciably greater than previously reported.<sup>13,14</sup> Significant reduction of (TPP)FeCl(ClO<sub>4</sub>) in the earlier work may serve to explain observed ortho and para-proton signals at 12.3 ppm and a meta-proton resonance at 5.8 ppm. These resonance values fall between those of spectra c and d in Figure 3 (for TPP(*p*-OCH<sub>3</sub>)FeCl(ClO<sub>4</sub>)) and could thus represent a mixture which is predominantly iron(III) porphyrin. Spectrum c of Figure 3 is more nearly representative for a pyrrole proton signal at 68.6 ppm (at 40 °C).<sup>13,14</sup> The fact that pyrrole and phenyl resonances do not rigorously follow the shift patterns in Figure 3 may be explained by the fact that both CDCl<sub>3</sub> and CD<sub>2</sub>Cl<sub>2</sub> solvents (with perhaps differing levels of reduction) were employed in the earlier study for observation of the two sets of signals.

Assignment and measurement of isotropic shift values is obviously of importance in attempting to understand the electronic structure of oxidized iron porphyrin species. Isotropic shift values for phenyl protons are surprisingly large, and are larger than those for any paramagnetic metal tetraphenylporphyrin complex yet examined. The contact shift contribution must be predominant, as dipolar shifts for ortho-, meta-, and para-phenyl protons would be in the same direction. Moreover, a  $\pi$ -contact shift mechanism for unpaired spin transfer in phenyl groups is demonstrated by (1) alternation in the shift direction around the phenyl ring, (2) ortho- and para-proton shifts of the same magnitude, and (3) alternation in shift direction for carbon-13 and attached proton signals. Observation of such large  $\pi$ -contact spin density at phenyl positions is unprecedented for simple paramagnetic metal tetraphenylporphyrin complexes as a consequence of phenyl groups lying approximately orthogonal to the porphyrin plane.<sup>57</sup> The large isotropic shifts are overall suggestive of porphyrin  $\pi$ -cation radical character. This is demonstrated by estimation of the NMR isotropic shift expected from the ESR ortho-phenyl electron-nuclear coupling constant of  $A^H = 0.316$  G (0.88 MHz) for the (TPP)Zn(ClO<sub>4</sub>)  $\pi$ -cation radical species.<sup>60</sup> An absolute isotropic shift of 23 ppm at 299 K is thus obtained from the following relationship (downfield shifts are given positive sign).<sup>61</sup>

$$\frac{\Delta H^{\text{iso}}}{H} = A^H \frac{\gamma_e}{\gamma_H} \frac{g\beta S(S+1)}{3kT}$$

Neglecting any shift contribution from the paramagnetic metal center, an absolute isotropic shift of 23 ppm translates into possible chemical shift values of 31 (downfield) or -15 ppm (upfield). This 31-ppm value is to be compared with an observed ortho-proton resonance at 36 ppm for (TPP)FeCl(ClO<sub>4</sub>). The comparison is complicated, however, by a comparable isotropic NMR shift for the para-phenyl proton signal. Earlier deuterium substitution experiments revealed that the para-phenyl proton of (TPP)Zn(ClO<sub>4</sub>) contributed to the hyperfine line widths in the ESR spectrum.<sup>32</sup> Although a coupling constant was not calculated for the para-phenyl proton, the value was judged to be less than for the ortho proton.

A radical center is normally expected to exhibit an ESR spectrum and induce extreme broadening of NMR resonances.

However, proximity of the paramagnetic iron atom should promote electronic relaxation to yield at best a very broad ESR spectrum and NMR signals which are not excessively broadened. Therefore, observation of well-defined NMR resonances does not necessarily preclude radical character in the species.

Two  $\pi$ -cation radical types have been characterized for metalloporphyrins.<sup>1,7,31-35</sup> The  $a_{2u}$  radical exhibits large spin density at the bridging meso-carbon and at pyrrole nitrogen atoms. Through a spin polarization mechanism the spin density at the meso-carbon atom could be readily transferred to an attached phenyl group. Little change in pyrrole proton isotropic shifts of (TPP)FeCl upon oxidation is reasonable based on the knowledge that the  $a_{2u}$  radical places little spin density at this position.

The oxidized OEP complex, (OEP)FeCl(ClO<sub>4</sub>), on the other hand, is better described as having  $a_{1u}$  character. This radical type has spin density concentrated at pyrrole carbon atoms. Calculations show no spin density at meso positions, although a meso proton ESR coupling constant of 1.48 G is measured for (OEP)Mg(ClO<sub>4</sub>).<sup>1</sup> With the assumption that the spin density results from electron correlation effects, a coupling constant of this magnitude would correspond to a downfield NMR isotropic shift of 109 ppm (a meso-carbon spin density of 0.12 for the  $a_{2u}$  radical<sup>1</sup> would yield an upfield isotropic shift of 200 ppm for the meso proton). Unequivocal assignment of the meso-proton signal of (OEP)FeCl(ClO<sub>4</sub>) (Figure 5) reveals a 36 ppm downfield isotropic shift with respect to the parent (OEP)FeCl species. Although this shift pattern favors the expected  $a_{1u}$  formulation, it is probably simplistic to expect direct additivity of metal-centered and radical-centered isotropic shifts. Furthermore, the meso-proton signal of high-spin iron(III) porphyrins exhibits a large shift variation dependent on the number of axial ligands.<sup>63,64</sup>

For the iron porphyrins examined here, electron abstraction thus appears to be from a predominantly porphyrin-centered rather than a metal-centered molecular orbital. Molecular orbital calculations show that oxidation of a high-spin iron(III) porphyrin is expected to involve loss of an electron from an MO with  $d_{x^2-y^2}$  (coordinate system with axes through pyrrole nitrogen atoms) character.<sup>1</sup> The "d<sup>4</sup>" complex would be isoelectronic with the manganese(III) analogue and might be expected to exhibit similar NMR isotropic shift patterns. However, this is not the case. The (TPP)MnCl species exhibits an upfield pyrrole proton resonance<sup>65</sup> as a consequence of metal  $\pi$ -spin delocalization through singly populated  $d_{xz}$ ,  $d_{yz}$  orbitals. Comparison of known transition-metal electronic structures with porphyrin isotropic shift patterns<sup>57,66</sup> strongly indicates single population of  $d_{x^2-y^2}$  in (TPP)FeCl(ClO<sub>4</sub>). In this regard the large downfield pyrrole proton isotropic shift is thought to be associated with predominant  $\sigma$ -spin delocalization involving  $d_{x^2-y^2}$ . Proton NMR spectra of (OEP)FeCl(ClO<sub>4</sub>) and (OEP)MnCl also differ most strikingly in that the meso-proton signal is in a far upfield position in the former case and in a far downfield position in the latter.<sup>65</sup>

Mössbauer measurements reveal little perturbation of charge at the iron center following iron porphyrin oxidation. Isomer shift values decrease slightly for oxidized  $\mu$ -oxo dimers but actually increase with oxidation of monomeric species. Comparative values for well-characterized high-spin iron(IV) complexes are not available. For low-spin iron(IV) species isomer shifts (at 77 K) range from 0.03 mm/s for HRP compound II<sup>4</sup> to 0.29 mm/s for a dithiocarbamate complex.<sup>49</sup> Differences in quadrupole splittings and line widths for TPP(*p*-OCH<sub>3</sub>)FeCl and TPP(*p*-OCH<sub>3</sub>)FeCl(ClO<sub>4</sub>) are noted in Table II. Line width differences are striking in that liquid helium temperatures are normally required for high-resolution Mössbauer spectra of high-spin iron(III)

(60) Fajer, J.; Borg, D. C.; Forman, A.; Dolphin, D.; Felton, R. H. *J. Am. Chem. Soc.* **1970**, *92*, 3451-3459.

(61) (a) Jesson, J. P. "NMR of Paramagnetic Molecules"; La Mar, G. N., Horrocks, W. D., Holm, R. H., Eds.; Academic Press: New York, 1973; pp 1-52. (b) Kreilick, R. W. *Ibid.*, pp 595-626.

(62) (a) Felton, R. H. "The Porphyrins"; Dolphin, D., Ed.; Academic Press: New York, 1978; Vol. 5, pp 53-125. (b) Fajer, J.; Davis, M. S. *Ibid.*; Vol. 4, pp 197-256.

(63) Kurland, R. J.; Little, R. G.; Davis, D. G.; Ho, C. *Biochemistry* **1971**, *10*, 2237-2246.

(64) Budd, D. L.; La Mar, G. N.; Langry, K. C.; Smith, K. M.; Nayyir-Mazhir, R. *J. Am. Chem. Soc.* **1979**, *101*, 6091-6096.

(65) La Mar, G. N.; Walker, F. A. *J. Am. Chem. Soc.* **1975**, *97*, 5103-5107.

(66) Goff, H.; La Mar, G. N.; Reed, C. A. *J. Am. Chem. Soc.* **1977**, *99*, 3641-3646.

(67) Phillippi, M. A.; Goff, H. M., submitted for publication.



species. More efficient electron relaxation in the oxidized complex via radical-iron(III) interactions could serve to explain this observation. Mössbauer spectroscopy also provides additional characterization of redox and ligation homogeneity in the isolated products. This is illustrated for (TPP)FeCl(ClO<sub>4</sub>) which in our preparations was continually contaminated with an additional iron(III) porphyrin. Proton NMR spectra of the material submitted for Mössbauer analysis showed approximately 25% contamination by material identified as (TPP)Fe(ClO<sub>4</sub>).<sup>59</sup> Mössbauer spectra in Table II confirm both the identity and quantity of this contaminant as a consequence of distinctively large quadrupole splitting for the  $S = 3/2, 5/2$  spin-admixed (TPP)Fe(ClO<sub>4</sub>) complex.<sup>58</sup> Although some perturbation of isomer shift and quadrupole splitting parameters appear due to differing counterions, the more extensive Mössbauer study of (TPP)FeCl(SbCl<sub>6</sub>) corroborates our results for the oxidized perchlorate analogues.<sup>21</sup>

Results of solution magnetic measurements do not provide unequivocal description of the electronic structure. The 5.5- $\mu_B$  magnetic moment for TPP(*p*-OCH<sub>3</sub>)FeCl(ClO<sub>4</sub>) and (OEP)-FeCl(ClO<sub>4</sub>) is anomalous, in that it is higher than the spin-only value of 4.9  $\mu_B$  expected for an  $S = 2$  iron(IV) or strongly coupled high-spin iron(III)-radical combination. The value of 5.5  $\mu_B$  is likewise not representative of an uncoupled  $S = 5/2 + S = 1/2$  system which should have a value of 6.16  $\mu_B$ . Antiferromagnetic coupling of  $S = 5/2$  and  $S = 1/2$  centers with  $J \approx -50$  cm<sup>-1</sup> would serve to explain the ambient temperature 5.5- $\mu_B$  value. However, a coupling constant of this magnitude would be associated with decreased magnetic moments at lower temperature. Temperature dependence is not apparent over the accessible range of 299–218 K, where the magnetic moment remains invariant at  $5.5 \pm 0.1 \mu_B$ . Moreover, a  $J \approx -50$  cm<sup>-1</sup> value would induce significant nonlinearity in the Curie law plots in Figure 4. Thus, if antiferromagnetic coupling is to be invoked, a  $|J|$  value considerably smaller than 50 cm<sup>-1</sup> or larger than perhaps 200 cm<sup>-1</sup> must be assumed. It is important to note that strong antiferromagnetic coupling between the low-spin iron(IV) center and the porphyrin radical is not the case for HRP compound I.<sup>4</sup> Explanation of the unusual magnetic moment remains elusive but could well be found in unusual electron correlation effects. Significant nonzero Curie intercepts for those phenyl resonances (ortho and para) with large radical-like spin density suggest second-order magnetic effects which are temperature dependent but not apparent over the 299–218 K range. It should be noted that solid-state magnetic measurements over the temperature range 5–300 K exhibit Curie law behavior with  $\mu = 5.1 \mu_B$ .<sup>21</sup> On this basis Gans et al. concluded that strongly coupled  $S = 5/2$  and  $S = 1/2$  centers define an  $S = 2$  state for (TPP)FeCl(SbCl<sub>6</sub>).<sup>21</sup>

Additional information favoring the radical character of oxidized products is found in the oxidation potentials for high-spin iron(III) porphyrin complexes and the infrared spectra of oxidized iron porphyrins. Oxidation potentials are essentially constant at  $1.10 \pm 0.02$  V vs. SCE for some 12 (TPP)FeX species.<sup>20</sup> Variation in the charge and ligand field character of X<sup>-</sup> is known to affect the iron electronic structure, spectroscopic properties, and thermodynamic binding properties. The surprising independence of oxidation potentials on the nature of X<sup>-</sup> is thus consistent with (but does not prove) that oxidation is porphyrin centered. Appearance of a new, strong infrared band in the 1280-cm<sup>-1</sup> region of oxidized metal tetraphenylporphyrin complexes seems to be diagnostic of porphyrin-centered oxidation. This band appears in the infrared spectrum of the known  $\pi$ -cation radical (TPP)-Zn(ClO<sub>4</sub>), as well as in all the spectra of oxidized (TPP)Fe complexes reported here. Deuterium substitution experiments confirm that the diagnostic band is associated with porphyrin core vibrations.<sup>44</sup>

Moderately strong metal-metal antiferromagnetic coupling in ( $\mu$ -oxo)iron porphyrin dimers further complicates elucidation of the detailed electronic structure of oxidized species. Radical character is apparent in significant isotropic shifts of TPP phenyl resonances (which alternate in sign around the ring). Phenyl isotropic shifts for [(TPP)Fe]<sub>2</sub>O are less than 0.4 ppm, whereas values range from 4–6 ppm for [(TPP)Fe]<sub>2</sub>O(ClO<sub>4</sub>). Mössbauer results support retention of iron(III) character in oxidized dimers, and infrared measurements seemingly point to a  $\pi$ -cation radical center. Partial coupling of radical spins through the  $\mu$ -oxo linkage must be invoked, however, to explain sizeable decreases in phenyl isotropic shifts for dimeric vs. monomeric products.

Large phenyl shifts are observed for the TPP(2,4,6-CH<sub>3</sub>)FeCl species doubly oxidized by *m*-chloroperoxybenzoic acid.<sup>15b</sup> However, the porphyrin meta-phenyl proton signal is in a far downfield position, unlike the upfield-shifted meta-phenyl signal of (TPP)FeCl(ClO<sub>4</sub>). A downfield isotropic shift of 60 ppm at -77 °C would correspond to a value of 39 ppm at 26 °C. This value is of greater magnitude than the 20-ppm upfield isotropic shift for (TPP)FeCl(ClO<sub>4</sub>). A complete explanation for changes in signs and magnitudes for the two radical species is not yet available but may well be based on population of d<sub>z<sup>2</sup></sub> and/or d<sub>x<sup>2</sup>-y<sup>2</sup></sub> orbitals. The oxidized TPP(2,4,6-CH<sub>3</sub>)FeCl complex appears to have an iron(IV) oxidation state,<sup>15a</sup> whereas (TPP)FeCl(ClO<sub>4</sub>) is best described as a high-spin iron(III) species. The d<sub>x<sup>2</sup>-y<sup>2</sup></sub> orbital is expected to be depopulated in the iron(IV) state. The bis(imidazole) adduct of (TPP)FeCl(ClO<sub>4</sub>), generated in situ at low temperature, is best formulated as a low-spin iron(III) porphyrin  $\pi$ -cation radical and accordingly has vacant d<sub>z<sup>2</sup></sub> and d<sub>x<sup>2</sup>-y<sup>2</sup></sub> orbitals.<sup>67</sup> Consistent with the d-orbital occupation hypothesis, the signs of phenyl proton isotropic shifts for the oxidized low-spin complex are reversed with respect to the high-spin precursor. Thus, the downfield meta-phenyl signal of (TPP)Fe(Im)<sub>2</sub><sup>2+</sup> follows in direction (if not in magnitude) that of oxidized TPP(2,4,6-CH<sub>3</sub>)-FeCl.

Oxidation of iron(III) porphyrin-anion complexes yields products better formulated as iron(III) porphyrin  $\pi$ -cation radicals rather than iron(IV) porphyrins. This observation does not, however, challenge formulation of iron(IV) intermediates in hemoproteins. Rather it supports the presumed necessity for an oxo or hydroxo ligand for stabilization of metal-centered oxidation. Radical-like compounds characterized in this work are in a sense more appropriate models for the putative  $\pi$ -cation radical compound I of HRP. Fundamental questions of oxo or other ligand stabilization of the iron(IV) state and involvement in oxidase reactions remain to be answered. Continued systematic preparation of appropriate model iron porphyrin compounds is directed at answering these questions.

**Acknowledgment.** Support from NSF Grant CHE 79-10305 and NIH Grant GM 28831-01 is gratefully acknowledged. We wish to thank Professor D.N. Hendrickson of the University of Illinois for providing Mossbauer measurements, and Professor R.E. Coffman of this Department for assistance with ESR determinations.

**Registry No.** [(TPP)Fe]<sub>2</sub>O(ClO<sub>4</sub>)<sub>2</sub>, 72319-58-5; [(TPP)Fe]<sub>2</sub>O, 12582-61-5; [TPP(*p*-OCH<sub>3</sub>)Fe]<sub>2</sub>O(ClO<sub>4</sub>)<sub>2</sub>, 79633-64-0; [(TPP)Fe]<sub>2</sub>O(ClO<sub>4</sub>), 79622-53-0; [(TPP)(*p*-OCH<sub>3</sub>)Fe]<sub>2</sub>O(ClO<sub>4</sub>), 80766-28-5; [(OEP)Fe]<sub>2</sub>O(ClO<sub>4</sub>), 82963-18-6; [(OEP)Fe]<sub>2</sub>O, 82978-79-8; TPP(*p*-OCH<sub>3</sub>)FeCl(ClO<sub>4</sub>), 79623-69-1; TPP(*p*-OCH<sub>3</sub>)FeCl, 36995-20-7; TPP-FeCl(ClO<sub>4</sub>), 79623-66-8; (OEP)FeCl(ClO<sub>4</sub>), 82963-19-7; [TPP(*p*-OCH<sub>3</sub>)Fe]<sub>2</sub>O, 37191-17-6; [TPP(*m*-CH<sub>3</sub>)Fe]<sub>2</sub>O, 51799-86-1; [TPP(*m*-CH<sub>3</sub>)Fe]<sub>2</sub>O(ClO<sub>4</sub>), 83044-12-6; [TPP(*o*-CH<sub>3</sub>)Fe]<sub>2</sub>O, 51909-24-1; [TPP(*o*-CH<sub>3</sub>)Fe]<sub>2</sub>O(ClO<sub>4</sub>), 83044-14-8; [(ETIO)Fe]<sub>2</sub>O, 54348-75-3; [(ETIO)Fe]<sub>2</sub>O(ClO<sub>4</sub>), 83060-65-5; iron(III) tetraphenylporphyrin chloride, 16456-81-8; iron(III) octaethylporphyrin chloride, 28755-93-3.